Critical magnetic behavior of ferromagnetic $CdCr_2S_4$

V. Tsurkan,[1,2] D. Ehlers,[1] V. Felea,[2] H.-A. Krug von Nidda,[1] and A. Loidl[1]

[1]*Experimental Physics 5, Center for Electronic Correlations and Magnetism, University of Augsburg, 86159 Augsburg, Germany*

[2]*Institute of Applied Physics, Academy of Sciences of Moldova, MD-2028 Chisinau, Republic of Moldova*

(Received 28 June 2013; revised manuscript received 1 October 2013; published 21 October 2013)

The critical magnetic behavior of the colossal magnetocapacitive spinel $CdCr_2S_4$ is revisited. Magnetization and susceptibility of single-crystalline samples measured in the temperature range 68–120 K were analyzed by the kink-point method, the modified Arrott plots, the Kouvel-Fisher method, ln M versus ln $H_{\rm eff}$, and the scaling analysis. We show that the critical exponents $\beta = 0.365$ and $\gamma = 1.387$ of the three-dimensional (3D) Heisenberg model describe the magnetic critical behavior only in the asymptotic region. Outside the asymptotic region, the values of β are reduced and those of γ are increased. We provide experimental evidence that the critical behavior of $CdCr_2S_4$ follows that expected for an ideal 3D Heisenberg system, however, in an unusual narrow window of temperature and in low magnetic fields only.

DOI: 10.1103/PhysRevB.88.144417 PACS number(s): 75.40.Cx, 65.40.Ba, 65.40.De, 75.50.Pp

I. INTRODUCTION

Ferromagnetic (FM) $CdCr_2S_4$ belongs to a family of chalcogenide spinels that are prominent for a rich variety of physical phenomena, including colossal magnetoresistance, giant redshift of the absorption edge, magnetic field-induced structural transformations, multiferroicity, spin and orbital frustration, etc., which result from strong electronic correlations combined with a strong coupling of structural and electronic degrees of freedom.[1,2] The discovery of colossal magnetocapacitance in FM $CdCr_2S_4$[3] stimulated the interest in magnetic spinels also as potential multiferroics, promising for spintronic applications beside the colossal magnetoresistance effect. Other multiferroics with spinel structure known thus far, e.g., $ZnCr_2Se_4$, $HgCr_2S_4$, and $CoCr_2O_4$, exhibit complex spiral or cycloid spin configurations with either antiferromagnetic or nearly compensated ferrimagnetic ground states.[4–6] The observation of the multiferroic properties in $CdCr_2S_4$, a compound with apparent cubic symmetry and simple collinear ferromagnetic spin arrangement, is in obvious contrast to the above-mentioned spinel multiferroics and was largely debated.[7–9] Subsequent studies[10,11] confirmed the ferroelectric behavior of $CdCr_2S_4$ and showed the possibility of magnetization modulation by application of an electric field.[11] Recent high-resolution x-ray powder diffraction[12] has established the dynamical off-centering of the octahedral Cr ions caused by the presence of simultaneous polar and magnetic nanoclusters. They also demonstrated that ultraslow displacement dynamics of Cr^{3+}ions precedes the recently reported $Fd\bar{3}m$ to non-centrosymmetric $F\bar{4}3m$ structural phase transition provided by Raman studies of high-quality single crystals grown by bromine transport.[13]

Not only the multiferroic behavior of $CdCr_2S_4$ was controversially discussed, but also the magnetic properties seem to be rather unusual. Recent FM resonance studies revealed an anomalous magnetic anisotropy that appeared below 20 K.[14] The muon spin rotation experiments reported on the observation of an anomaly in the paramagnetic spectra below 150 to 100 K, coinciding with a possible structural transformation and on persistent and strong spin fluctuations towards the lowest temperatures.[15] Finally, using ac susceptibility, dc magnetization, and electron-spin resonance, Luo *et al.*[16] analyzed the critical behavior of $CdCr_2S_4$ polycrystals and reported that the values of the critical exponents deviate notably from those of the three-dimensional (3D) Heisenberg model. The observed abnormal magnetic behavior of $CdCr_2S_4$ was attributed to a formation of correlated magnetic polarons and strong spin-phonon coupling, which was suggested to be the reason for the polar ground state.

In the present paper, we readdressed the problem of the critical magnetic behavior by a study of single-crystalline $CdCr_2S_4$ samples using well-established methods to analyze the magnetic isotherms, which earlier were successfully applied to get reliable information on the critical behavior of various magnetic systems.[17]

II. EXPERIMENTAL DETAILS

Single crystals of $CdCr_2S_4$ have been grown by chemical transport reactions from preliminary synthesized polycrystalline material prepared by solid-state reactions from high-purity (99.99% and better) elements. Details of the sample preparation and compositional control of the single crystals were presented in Ref. 10. For the analysis, we selected samples from the same batch that show the pronounced magnetocapacitive behavior described in Ref. 3. The magnetic properties of the samples have been studied by means of a superconducting quantum interference device magnetometer (Quantum Design, MPMS-7) in the temperature range $4.2 \leqslant T \leqslant 130$ K and in magnetic fields up to 12 kOe. For the measurements of magnetization, isotherms temperature steps of 0.1 and 0.2 K were used in the critical region. Critical temperature and critical exponents were determined by commonly used techniques, i.e., the kink-point method, the modified Arrott plots, the Kouvel-Fisher method, ln M versus ln $H_{\rm eff}$, and the scaling analysis, justified in Ref. 17. The effective field $H_{\rm eff}$ was calculated by subtracting the demagnetizing field from the applied field. The demagnetizing factor was obtained from the low-field ($\leqslant$50 Oe) magnetization data in the FM state.

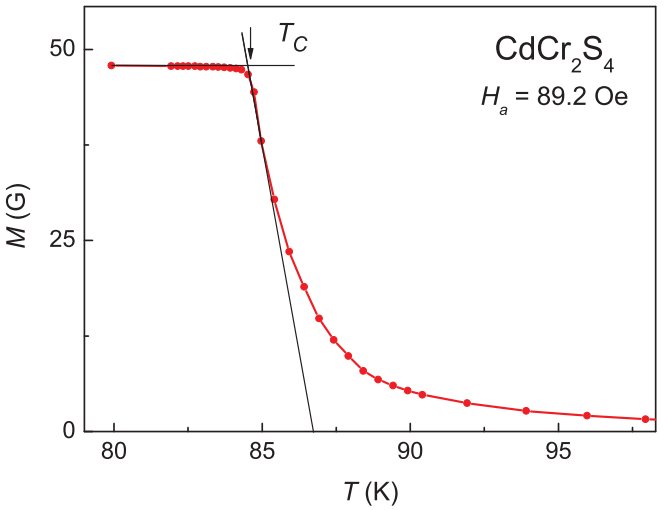

FIG. 1. (Color online) Temperature dependence of the magnetization M for single-crystalline $CdCr_2S_4$ measured on cooling in a field of 89.2 Oe.

III. EXPERIMENTAL RESULTS AND DISCUSSION

In Fig. 1 the temperature dependence of the magnetization M is presented for single-crystalline $CdCr_2S_4$ measured on cooling in a field of 89.2 Oe. It shows a sharp kink at a temperature of 84.6 K, identifying the value of the Curie temperature T_C. The width of the transition estimated using the criteria 90/10% is about 1.8 K. The ac susceptibility measured at different frequencies shows a similar sharp transition with a kink at 84.7 K for zero dc field, in good correlation with the static data (see Supplemental Material in Ref. 18).

The spontaneous magnetization M_s and the initial susceptibility χ_0 were obtained from modified Arrott plots defined as[19]

$$(H_{\text{eff}}/M)^{1/\gamma} = k_1 t + k_2 M^{1/\beta}. \quad (1)$$

Here H_{eff} is the internal field $H_{\text{eff}} = H_a - NM$, H_a is the applied field, N is the demagnetizing coefficient, β and γ are the critical exponents describing, respectively, the behavior of the spontaneous magnetization M_s and of the initial susceptibility χ_0, and t is the reduced temperature, $t = |(T/T_C - 1)|$.

In Fig. 2, the modified Arrott plots for the single-crystalline $CdCr_2S_4$ are shown in the vicinity of the magnetic phase-transition temperature T_C. The plots were constructed from the magnetization isotherms measured with minimal temperature steps of 0.1 and 0.2 K. The plots are drawn using the 3D Heisenberg values of the critical exponents $\beta = 0.365$ and $\gamma = 1.387$.[20] With these exponents, the Arrott plots present a set of almost straight lines, however, only for a rather restricted field range. In the full range of the applied magnetic fields, the Arrott plots are essentially nonlinear (Fig. 3). We note that the commonly used extrapolation procedure, which prioritizes high-field data, cannot be applied in the present case. Indeed, linear extrapolation of the high-field data for the isotherm at 86.4 K gives a positive intercept on the M^1/β axis, indicating a FM state. However, ferromagnetism of the sample is definitely no more long-range ordered as can be concluded from the temperature dependence of the magnetization of

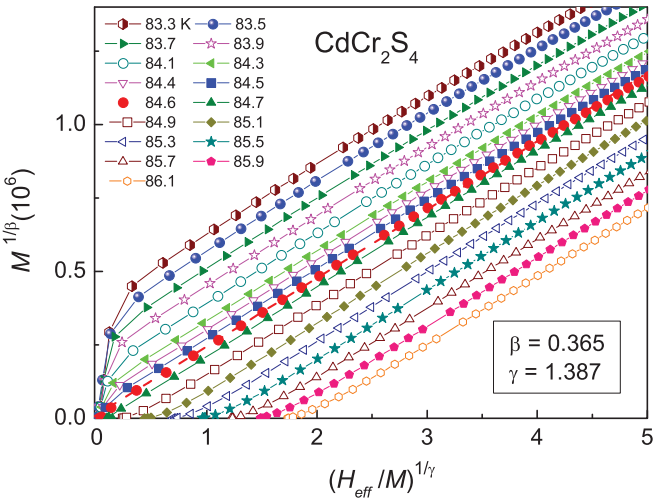

FIG. 2. (Color online) Modified Arrott plots for a $CdCr_2S_4$ single-crystal (M in G; H_{eff} in Oe) in a restricted range of applied magnetic fields (0–1850 Oe). The dashed line represents the least-square fit to the isotherm at 84.6 K. The solid lines are guides to the eye.

Fig. 1. Returning to the set of straight-line-like Arrott plots shown in Fig. 2, one can notice that the isotherm most closely passing through the origin, which defines the critical isotherm, corresponds to the isotherm at 84.6 K and perfectly correlates with the value of the Curie temperature T_C determined by the kink-point method (Fig. 1). Note also that linear extrapolation of the high-field part of the isotherm of our sample at 85.5 K, constructed with the exponents values $\beta = 0.33$ and $\gamma = 1.44$ taken from the Ref. 16, gives an almost zero intercept that can be associated with the Curie temperature (see Supplemental Material in Ref. 21). This value coincides with the value of the Curie temperature of 85.6 ± 0.3 K, defined in Ref. 16. This coincidence may be not accidental but represents the effect of the high-field extrapolation applied in particular to the systems with strong magnetoelastic coupling, e.g., $CdCr_2S_4$ in this case. Therefore, we conclude that fitting of the low-field data

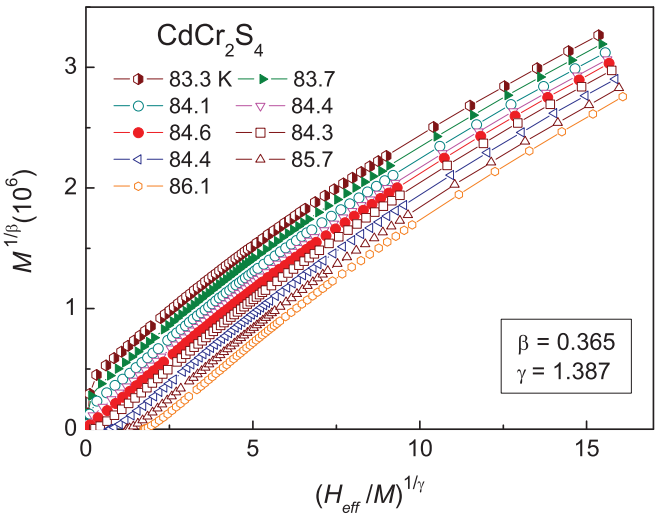

FIG. 3. (Color online) Modified Arrott plots for a $CdCr_2S_4$ single crystal in the full range of the applied magnetic fields. For clarity, several isotherms are omitted compared to Fig. 2.

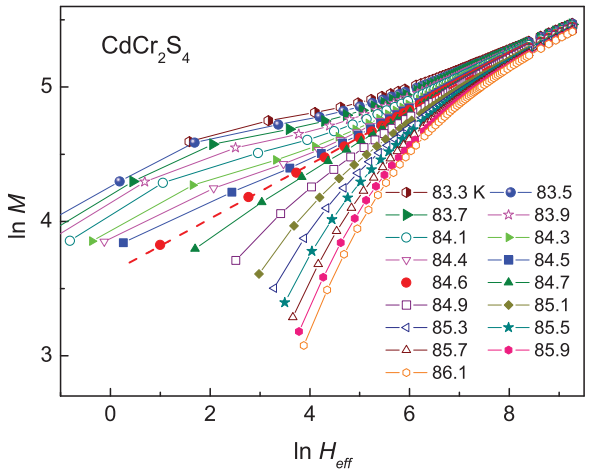

FIG. 4. (Color online) The ln M versus ln H_{eff} isotherms in the vicinity of the Curie temperature for single-crystalline $CdCr_2S_4$ (M in G; H_{eff} in Oe). The dashed line represents the least-square fit to the isotherm at 84.6 K. The solid lines are guides to the eye.

is more reasonable providing consistent critical temperatures determined in different independent ways.

In case of such strong nonlinearities of the Arrott plots, it is necessary to justify the range of the fields for the extrapolation. For this, it is instructive to analyze the plot M versus H_{eff}, which is commonly used for calculating the third critical exponent δ defined as

$$H_{\text{eff}} = k_3 M^{\delta}. \tag{2}$$

Figure 4 shows the magnetization isotherms versus internal field H_{eff} on a double logarithmic scale in the vicinity of the Curie temperature. The smallest deviation from the straight line is found for the isotherm at 84.6 K, being the critical isotherm, in agreement with the above-mentioned observations. The least-square fit to the data for this isotherm resulted in a value $\delta = 5.05 \pm 0.02$ for the complete field range. This value is slightly higher than $\delta = 4.8$ of the 3D Heisenberg model. Keeping in mind that the full-field range cannot be used for the evaluation of critical exponents, as already noticed by the strong nonlinearity of the Arrott plots (Fig. 3), we calculated δ by continuously reducing the range of fields used for the fitting procedure. The smallest value of $\delta = 4.94 \pm 0.01$ obtained in such a way corresponds to an effective field H_{eff} of 1600 Oe. This field is considered as an upper limit for the extrapolation of the Arrott plots in the vicinity of the Curie temperature for extraction of the spontaneous magnetization M_s and of the initial susceptibility χ_0. In this field range, the deviations of the isotherms from the straight line in the modified Arrott plots are insignificant compared to those for the full-field range, as can be clearly seen in Fig. 2.

In Figs. 5(a) and 6(a), the temperature dependence of the spontaneous magnetization M_s and of the initial susceptibility χ_0 determined by such an extrapolation are presented. Further processing of M_s and χ_0 was performed using the Kouvel-Fisher method[22] by constructing the functions $Y(T)$ and $X(T)$ defined by the expressions

$$Y(T) = M_s^{-1} \big/ \left(dM_s^{-1}/dT\right), \tag{3}$$

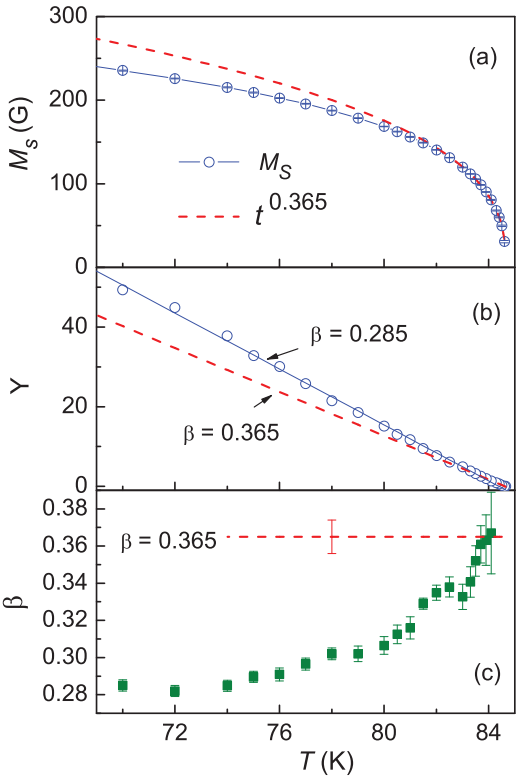

FIG. 5. (Color online) Temperature dependencies of the spontaneous magnetization M_s (a), of the Kouvel-Fisher function Y (b), and of the exponent β. Dashed lines show the dependencies expected for the exponent $\beta = 0.365$. The error bar on the dashed theoretical line in the frame (c) shows the range of deviations of β for the 3D Heisenberg model calculated by different methods according to Ref. 24.

and

$$X(T) = \chi_0^{-1} \big/ \left(d\chi_0^{-1}/dT\right). \tag{4}$$

The temperature dependence of the $Y(T)$ and $X(T)$ functions are shown in Figs. 5(b) and 6(b), respectively. The values of β and γ were determined from the inverse slope of these functions and are presented in Figs. 5(c) and 6(c). From the obtained data, it is evident that the Heisenberg exponents describe well the temperature dependencies of the spontaneous magnetization M_s and of the initial susceptibility χ_0 only in a restricted temperature range close to T_C. The critical range where the deviations of the data calculated using the values of the critical exponents are larger than the accuracy of the extrapolation of the data from the Arrott plots, is estimated as $t \approx 1.6 \cdot 10^{-2}$ for temperatures below T_C and $t \approx 6 \cdot 10^{-2}$ for temperatures above T_C. Outside the critical range, the exponent β shows a tendency for decreasing, while the exponent γ increases. Note that the values of the exponents β and γ reported in Ref. 16 represent their values outside the critical range. The Arrott plots constructed with the values of β and γ, taken from Ref. 16, show significantly larger deviations from the straight lines (see Supplemental Material in Ref. 23) than those shown in Fig. 2. Outside the critical range, these exponents are only effective ones, averaged over a larger temperature region. It is also noteworthy that outside the critical temperature range, a similar tendency for the deviation of the exponent values from those of the 3D Heisenberg model

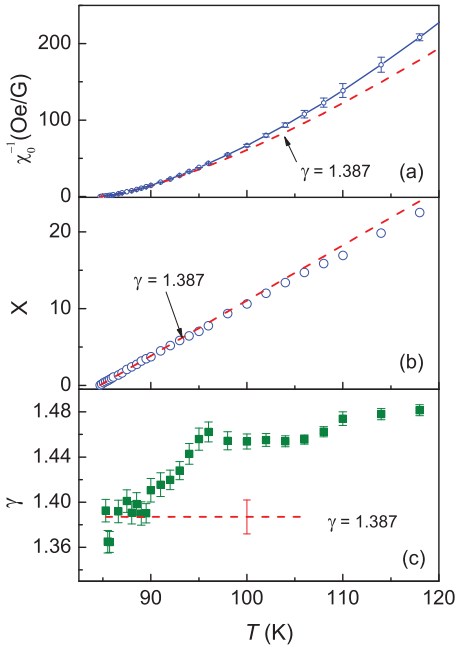

FIG. 6. (Color online) Temperature dependencies of the initial susceptibility χ_0 (a), of the Kouvel-Fisher function X (b), and of the exponent γ. Dashed lines show the dependencies expected for the exponent $\gamma = 1.387$. The error bar on the dashed theoretical line in the frame (c) shows the range of deviations of γ for the 3D Heisenberg model calculated by different methods according to Ref. 24.

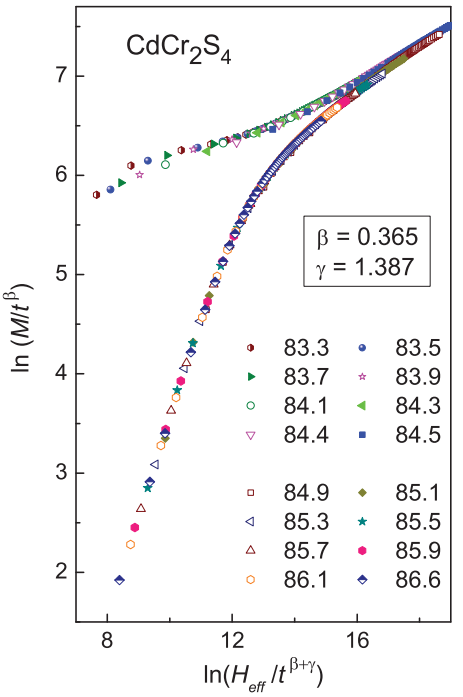

FIG. 7. (Color online) The scaling plots for $CdCr_2S_4$ single crystals (M in G; H_{eff} in Oe) constructed using the values of the critical exponents of the 3D Heisenberg model.

has been reported earlier for a large number of magnetic systems, including spinel ferrites (see critical review presented in[17]). Our results establish such a behavior also for $CdCr_2S_4$.

An additional point to be emphasized is that the values of the critical exponents satisfy the Widom scaling relation[25]

$$\gamma = \beta\,(\delta - 1)\,. \tag{5}$$

The relation (5) assumes the data in the critical region to obey the scaling equation of state

$$m = f_{\pm}(h) \tag{6}$$

that describes two universal curves for $T < T_C$ and for $T > T_C$. Here, $m = M/t^\beta$ and $h = H_{\text{eff}}/t^{\beta+\gamma}$ are the scaled magnetization and the scaled field, respectively. In Fig. 7 the scaling plots $\ln(M/t^\beta) = f\{\ln(H_{\text{eff}}/t^{\beta+\gamma})\}$ for the $CdCr_2S_4$ single crystal are shown. The collapse of these dependences on two branches for $T < T_C$ and for $T > T_C$ with the relatively small scattering of the data has been obtained. Thus, the 3D Heisenberg values of the critical exponents in $CdCr_2S_4$ are again confirmed.

Finally, we would like to note that $CdCr_2S_4$ behaves as an ideal Heisenberg ferromagnet only in relatively low magnetic fields. The observed strong nonlinearity of the modified Arrott plots at high fields signifies an essential feature of this compound. It is clear that high fields can drive a system away from the critical range. However, it is unclear why this effect is so strong in $CdCr_2S_4$. For example, in the related ferrimagnetic spinel compound $MnCr_2S_4$, which exhibits a close value of the transition temperature (66 K) and shows a perfect Heisenberg critical behavior, the Arrott plots are strictly linear up to the highest magnetic fields.[26]

A strong sensitivity of the magnetism of $CdCr_2S_4$ to external magnetic fields is an intrinsic property of this compound. As one can see from the magnetization and specific heat data shown in Figs. 8(a) and 8(b), already magnetic fields below 1 T produce significant changes of these quantities. A possible explanation of the strong sensitivity of the magnetic system of $CdCr_2S_4$ can be provided by thermal expansion and magnetostriction effects. In Fig. 8(c), we show the temperature dependence of the relative change of the sample length $\Delta L/L$ for fields of zero and 50 kOe. The measurements were done on a single-crystalline sample from a similarly prepared batch, which also shows the colossal magnetocapacitive properties and relaxor ferroelectric behavior like the sample described above. In zero field, on decreasing temperatures in the paramagnetic range from 250 to 180 K, the thermal expansion exhibits a continuous decrease that can be ascribed to an anharmonic behavior usually observed in solids. Below 180 K, the rate of decrease of $\Delta L/L$ becomes smaller and shows a broad minimum at around 120 K. On further decreasing temperatures, the sample exhibits a strong negative thermal expansion with an additional pronounced anomaly at the Curie temperature as presented in the inset of Fig. 8(c). The application of the magnetic field has a considerable influence on the thermal expansion, suppressing the anomaly at T_C and shifting the minimum in $\Delta L/L$ to higher temperatures. Above 200 K, the influence of the magnetic field on the thermal expansion is insignificant. It must be mentioned that the range below 200 K down to 120 K, where the pronounced changes in the thermal expansion are evident, coincides with the range where significant FM spin fluctuations appear. This is just the range where the simultaneous polar and magnetic nanoclusters develop[12] and relaxor ferroelectric behavior is found.[3] This correlation

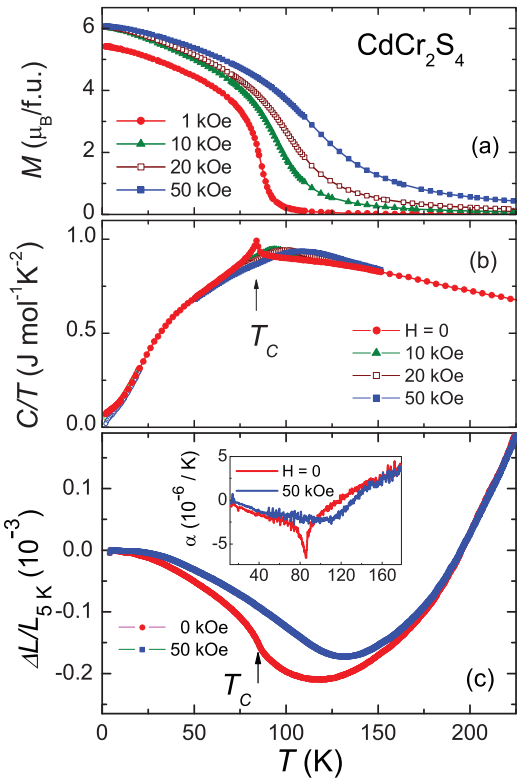

FIG. 8. (Color online) Temperature dependencies of the magnetization (a), of the specific heat (b), and of the relative change of the sample length $\Delta L/L$ normalized to its value at 5 K (c) for the fields of 0 and 50 kOe. The inset in the frame (c) shows the temperature dependence of the thermal expansion coefficient $\alpha = 1/L(dL/dT)$ in the range close to T_C.

suggests that the underlying physical mechanism that produces the colossal magnetocapacitance and relaxor ferroelectric behavior is connected with the strong magnetoelastic coupling in $CdCr_2S_4$. In high magnetic fields, the distance between the magnetic ions can be changed due to magnetostriction effect, which, in turn, can change the internal magnetic fields and modify the magnetic behavior, explaining the observed strong nonlinearity of the magnetic isotherms at high fields.

IV. CONCLUSIONS

In conclusion, we performed a detailed analysis of the magnetization and susceptibility of the single crystalline $CdCr_2S_4$ sample measured with smallest available temperature steps close to the Curie temperature using well-established techniques of data processing, including the kink-point method, the modified Arrott plots, the Kouvel- Fisher method, ln M versus ln H_{eff}, and the scaling analysis. All utilized techniques show a perfect agreement concerning the value of the transition temperature $T_C = 84.6$ K, and the values of the exponents in the critical range, thus confirming that the 3D Heisenberg model perfectly describes the critical magnetic behavior of this compound. However, we also provide experimental evidence that the 3D Heisenberg behavior only is valid in a very limited temperature range close to T_C and only in very low magnetic fields. We documented an unusual strong influence of external magnetic fields on magnetic fluctuations and on thermal expansion. The strong magnetoelastic coupling in $CdCr_2S_4$ could help to explain a number of structural anomalies observed in different experiments and may pay a decisive role in the formation of relaxor ferroelectricity.

ACKNOWLEDGMENTS

The authors thank Dana Vieweg and Thomas Wiedenmann for experimental support. This research has been supported by German Research Foundation (DFG) via Transregional Collaborative Research Center TRR 80 (Augsburg–Munich).

[1] R. P. van Stapele, in *Ferromagnetic Materials*, edited by E. P. Wohlfarth, Vol. 3 (North-Holland Publishing Company, Amsterdam, 1982), p. 603.
[2] V. Tsurkan, H.-A. Krug von Nidda, A. Krimmel, P. Lunkenheimer, J. Hemberger, T. Rudolf, and A. Loidl, Phys. Status Solidi A **206**, 1082 (2009).
[3] J. Hemberger, P. Lunkenheimer, R. Fichtl, H.-A. Krug von Nidda, V. Tsurkan, and A. Loidl, Nature (London) **434**, 364 (2005).
[4] H. Murakawa, Y. Onose, K. Ohgushi, S. Ishiwata, and Y. Tokura, J. Phys. Soc. Jpn. **77**, 043709 (2008).
[5] S. Weber, P. Lunkenheimer, R. Fichtl, J. Hemberger, V. Tsurkan, and A. Loidl, Phys. Rev. Lett. **96**, 157202 (2006).
[6] M. Mostovoy, Phys. Rev. Lett. **96**, 067601 (2006).
[7] G. Catalan and J. F. Scott, Nature (London) **448**, E4 (2007).
[8] J. Hemberger, P. Lunkenheimer, R. Fichtl, H.-A. Krug von Nidda, V. Tsurkan, and A. Loidl, Nature (London) **448**, E5 (2007).
[9] A. Loidl, S. Krohns, F. Schrettle, and P. Lunkenheimer, J. Phys.: Condens. Matter **20**, 191001 (2008).
[10] S. Krohns, F. Schrettle, P. Lunkenheimer, V. Tsurkan, A. Loidl, Physica B **403**, 4224 (2008).
[11] C. P. Sun, C. C. Lin, J. L. Her, C. J. Ho, S. Taran, H. Berger, B. K. Chaudhuri, and H. D. Yang, Phys. Rev. B **79**, 214116 (2009).
[12] G. N. P. Oliveira, A. M. Pereira, A. M. L. Lopes, J. S. Amaral, A. M. dos Santos, Y. Ren, T. M. Mendonça, C. T. Sousa, V. S. Amaral, J. G. Correia, and J. P. Araújo, Phys. Rev. B **86**, 224418 (2012).
[13] V. Gnezdilov, P. Lemmens, Yu. G. Pashkevich, Ch. Payen, K. Y. Choi, J. Hemberger, A. Loidl, and V. Tsurkan, Phys. Rev. B **84**, 045106 (2011).
[14] D. Ehlers, V. Tsurkan, H.-A. Krug von Nidda, and A. Loidl, Phys. Rev. B **86**, 174423 (2012).
[15] O. Hartmann, G. M. Kalvius, R. Wäppling, A. Günther, V. Tsurkan, A. Krimmel, and A. Loidl, Eur. Phys. J. B **86**, 148 (2013).
[16] X. Luo, Z. R. Yang, Y. P. Sun, X. B. Zhu, W. H. Song, and J. M. Dai, J. Appl. Phys. **106**, 113920 (2009).
[17] S. N. Kaul, J. Magn. Magn. Mater. **53**, 5 (1985).

[18]See Supplemental Material at http://link.aps.org/supplemental/10.1103/PhysRevB.88.144417 for temperature dependence of the ac susceptibility, Fig. 1SM.
[19]A. Arrott and J. E. Noakes, Phys. Rev. Lett. **19**, 786 (1967).
[20]J. C. Le Guillou and J. Zinn-Justin, Phys. Rev. B **21**, 3976 (1980).
[21]See Supplemental Material at http://link.aps.org/supplemental/10.1103/PhysRevB.88.144417 for the Arrott plots in the full range of the applied magnetic field, Fig. 2SM.
[22]J. S. Kouvel and M. E. Fisher, Phys. Rev. **136**, A1626 (1964).
[23]See Supplemental Material at http://link.aps.org/supplemental/10.1103/PhysRevB.88.144417 for the Arrott plots in the low-field range of the applied magnetic field, Fig. 3SM.
[24]M. Campostrini, M. Hasenbusch, A. Pelissetto, P. Rossi, and E. Vicari, Phys. Rev. B **65**, 144520 (2002).
[25]B. Widom, J. Chem. Phys. **43**, 3892 (1965).
[26]V. Tsurkan, M. Baran, A. Szewczyk, R. Szymczak, and H. Szymczak, J. Phys.: Condens. Matter **11**, 7907 (1999).